

A direct projection from superior colliculus to substantia nigra for detecting salient visual events

Eliane Comoli¹, Véronique Coizet¹, Justin Boyes², J Paul Bolam², Newton S Canteras³, Rachel H Quirk¹, Paul G Overton¹ & Peter Redgrave¹

Midbrain dopaminergic neurons respond to unexpected and biologically salient events, but little is known about the sensory systems underlying this response. Here we describe, in the rat, a direct projection from a primary visual structure, the midbrain superior colliculus (SC), to the substantia nigra pars compacta (SNc) where direct synaptic contacts are made with both dopaminergic and non-dopaminergic neurons. Complementary electrophysiological data reveal that short-latency visual responses in the SNc are abolished by ipsilateral lesions of the SC and increased by local collicular stimulation. These results show that the tectonigral projection is ideally located to relay short-latency visual information to dopamine-containing regions of the ventral midbrain. We conclude that it is within this afferent sensory circuitry that the critical perceptual discriminations that identify stimuli as both unpredicted and biologically salient are made.

Dopaminergic neurons located in the SNc and the ventral tegmental area respond to unexpected biologically salient stimuli, including those associated with reward, with a stereotyped short-latency (typically <100 ms), short-duration (~100 ms) increase in firing rate^{1,2}. This response has been observed in a variety of mammals including rat³, rabbit⁴, cat⁵ and monkey², and it has been studied mainly in the context of novelty^{6,7} and reward or reward-related stimuli². In the monkey, the response to a novel event rapidly habituates if it is not reinforced, as does the response to reward-related stimuli that can be predicted. When reward is predicted by an unexpected arbitrary stimulus (such as a tone or light), the phasic response of dopaminergic neurons gradually shifts from the primary reward to the predicting stimulus. However, if a predicted reward is withheld, dopaminergic neurons respond with a brief pause in firing, again with a latency of about 100 ms after the time of expected reward delivery. On the basis of these and more recent data⁸, the influential view has emerged that phasic responses of dopamine neurons signal a 'reward prediction error', which is used to adjust future behavioral response probabilities in reinforcement learning⁹. Simulated dopaminergic neuronal responses are an effective 'teaching signal' in several models of reinforcement learning^{10,11}.

The reward prediction error viewpoint makes two assumptions: (i) that a stimulus can be recognized as unpredicted (well supported¹²) and (ii) that a stimulus can be recognized as a reward or reward-related (less well supported^{6,7}). A caveat of these assumptions is that the perceptual analyses required to recognize an unexpected stimulus as 'reward' or 'reward-related' must rely on pre-attentive processing. For example, when an unpredicted visual event occurs, the latency to initiate a gaze shift to bring the event onto the fovea

(typically >150 ms) is almost always longer than the latency of the dopaminergic neuron response (~100 ms)⁶. Consequently, if dopaminergic neurons signal reward prediction error, the computations required to generate the response would have to be conducted *before* the animal switches its gaze to see fully what the stimulus is.

One strategy to elucidate the nature of the information contained in the dopamine signal is therefore to determine the perceptual properties of afferent sensory circuits. Here, we have sought to identify the pathways that can supply dopaminergic neurons with short-latency visual input. In the case of such stimuli, retinal projections to either the lateral geniculate–visual cortex system or the midbrain SC are the most likely sources of short-latency visual activation¹³. However, because response latencies in cortical regions engaged in feature detection and object recognition are typically longer than those of dopaminergic neurons¹⁴, extra-foveal cortical processing is unlikely to provide an invariant short-latency route to the ventral midbrain. In contrast, visual response latencies of neurons in the midbrain SC, a region specialized for the detection of unexpected salient events^{15,16}, are consistently less than those seen in dopaminergic neurons^{17,18}. Moreover, we have recently shown that chemical stimulation of the SC can evoke correlated burst activity in the substantia nigra and the ventral tegmental area¹⁹. Together, these data suggest that the SC may be the more plausible relay for mediating short-latency activation of dopaminergic neurons by visual stimuli. Our present results confirm this supposition, first by demonstrating a previously unreported direct anatomical projection between the SC and substantia nigra, and secondly by establishing that the SC is critical for short-latency visual activation of dopamine-containing regions of the ventral midbrain. Some of the present results have previously appeared in

¹Department of Psychology, University of Sheffield, Sheffield S10 2TP, UK. ²MRC Anatomical Neuropharmacology Unit, University of Oxford, Mansfield Road, Oxford OX1 3TH, UK. ³Department of Physiology and Biophysics, Institute of Biomedical Sciences, University of Sao Paulo, Sao Paulo, CEP 05508-900, Brazil. Correspondence should be addressed to P.R. (P.Redgrave@sheffield.ac.uk).

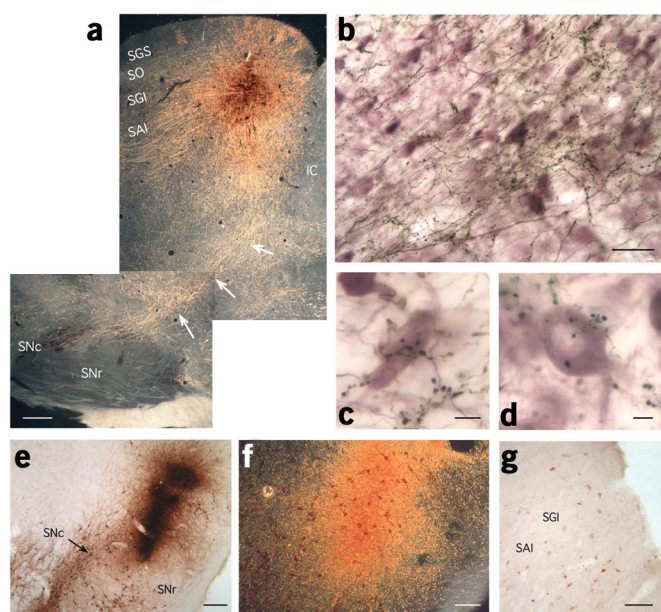


Figure 1 The tectonigral projection revealed by anterograde and retrograde tract tracing. (a) A darkfield photomontage of a parasagittal section of the rat midbrain illustrating an injection site of the anterograde tracer BDA in the caudal intermediate layers of the SC, with ventrally projecting tectonigral fibers (white arrows) directed to TH-positive regions (purple) of the SNc. (b) Tectonigral fibers with numerous boutons coursing rostrally (top-right to bottom-left) in a parasagittal section, running between TH-positive cells (purple) in SNc. (c) Tectonigral boutons in close association with a TH-immunopositive neuron in SNc. Note also the anterogradely labeled terminals in adjacent TH-negative regions. (d) Tectonigral boutons apposed to a TH-positive perikaryon in the ventral tegmental area. (e) An injection site of the retrograde tracer cholera toxin subunit b (CTb) in the lateral SNc in coronal section. (f) A darkfield photomicrograph of an adjacent section showing the injection site (orange) was centered on a region containing numerous TH-positive cells (purple). (g) Cells retrogradely labeled with CTb in the lateral intermediate layers of the SC in coronal section. Abbreviations in collicular layers: SGS, stratum griseum superficiale; SO, stratum opticum; SGI, stratum griseum intermediale; SAI, stratum album intermediale. Substantia nigra: SNc, pars compacta; SNr, pars reticulata. Scale bars: 0.5 mm (a), 30 μ m (b), 5 μ m (c,d), 200 μ m (e), 100 μ m (f,g).

abstract form (Coizet, V. *et al.*, *Soc. Neurosci. Abstr.* 28, 461.1, 2002 and Comoli, E. *et al.*, *Soc. Neurosci. Abstr.* 27, 68.11, 2001).

RESULTS

Anterograde tract tracing: light microscopy

To characterize the connections between the SC and dopaminergic neurons in the ventral midbrain, we used a combination of anterograde and retrograde tract-tracing techniques with tyrosine hydroxylase (TH) immunohistochemistry to identify dopaminergic structures. Injections of the anterograde tracers *Phaseolus vulgaris* leucoagglutinin (PHA-L) or biotinylated dextran amine (BDA) into the SC of the rat revealed a significant direct projection to the ipsilateral substantia nigra and ventral tegmental area (Figs. 1 and 3). The pathway descends vertically from the SC, through underlying reticular tissue, then curves rostrally to enter the caudal pole of SNc (Figs. 1a and 3a). Labeled fibers run the full rostro-caudal length of pars compacta (Fig. 1b), with some fibers entering the medially located ventral tegmental area at rostral levels (Fig. 3a). Throughout pars compacta (Fig. 1c) and the ventral tegmental area (Fig. 1d), axonal boutons were seen in close association with TH-positive perikarya and dendrites, as well as in regions devoid of TH immunostaining (Fig. 1b–d). Tectonigral fibers and boutons were also seen in regions of the caudal substantia nigra pars reticulata (SNr) that contain a ventral group of dopaminergic neurons²⁰ (Fig. 3a). Anterograde labeling was sparse or absent from non-dopaminergic regions of the SNr. Structures dorsally adjacent to the SNc, including zona incerta, also contained anterogradely labeled boutons and axons. At the light microscopic level, both PHA-L and BDA produced qualitatively and quantitatively similar anterograde labeling. In some

cases, however, neurons in the SNr were labeled with BDA, raising the possibility that some of the boutons observed in SNc may derive from local collaterals of retrogradely labeled nigroreticular neurons (see electron microscopy data below).

Anterograde tract tracing: electron microscopy

Electron microscopic analysis was carried out on tissue from four rats (two injected with PHAL and two with BDA). A total of 89/111 (80.2%) synaptic terminals, located mostly in the SNc, were confirmed as anterogradely labeled from the SC. There were two main classes. The first class comprised medium-size boutons (0.5–1.5 μ m in diameter) containing numerous round vesicles and occasional mitochondria. These boutons characteristically formed asymmetric synapses ($n = 54$) with both TH-positive ($n = 8$, Fig. 2a) and TH-negative dendrites ($n = 46$, Fig. 2b). The postsynaptic density was variable and was sometimes associated with post-junctional dense bodies. The

Figure 2 Axon terminals anterogradely labeled from the SC and forming synapses in SNc. (a,b) One type of anterogradely labeled terminal boutons (labeled 'b') form asymmetrical synapses (arrows) with TH-immunolabeled (a; TH-den) and unlabeled dendrites (b; den). (c,d) The second type of anterogradely labeled terminal boutons (b) are shown. This type formed symmetrical synapses (arrows) with TH-immunolabeled (c; TH-den) and unlabeled dendrites (d; den). Note the axon terminals that were not anterogradely labeled (*) in a and d. Scale bars, 0.5 μ m.

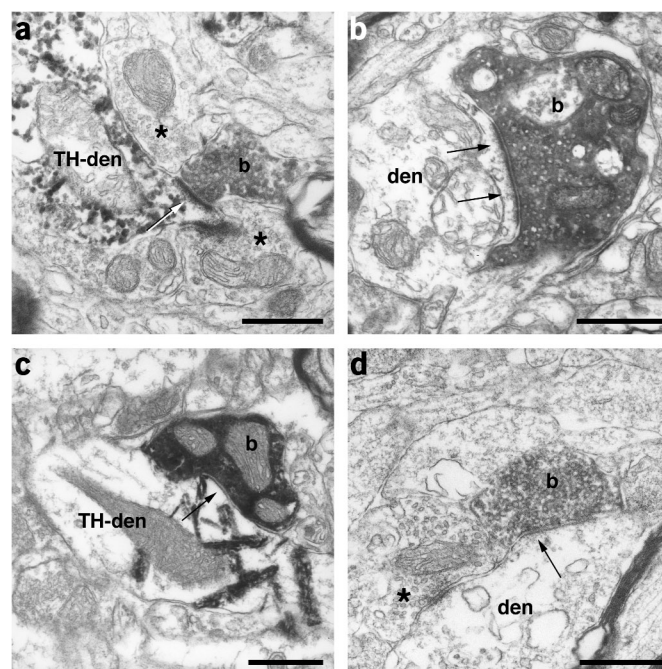


Table 1 Densities of anterogradely labeled boutons in SNc

SC injection site	Boutons in SNc per 300- μ m diameter field (mean \pm s.e.m.)	
	Medial	Lateral
Medial ($n = 3$) (1.4 mm from midline)	67.9 \pm 13.7	37.5 \pm 5.2
Lateral ($n = 4$) (2.9 mm from midline)	175.1 \pm 21.2	401.3 \pm 55.8

second class comprised medium-sized boutons (0.5–1.0 μ m in diameter) containing vesicles of variable shape and sometimes mitochondria, which formed symmetric synapses ($n = 26$) with both TH-positive ($n = 2$, Fig. 2c) and TH-negative ($n = 24$, Fig. 2d) dendrites. A further nine anterogradely labeled synaptic boutons could not be clearly categorized as forming symmetrical or asymmetrical synapses. A third class of labeled boutons ($n = 22$, 19.8%) also formed symmetric synapses with both TH-positive ($n = 16$) and TH-negative structures ($n = 6$), but were larger (up to 2.5 μ m in diameter) and usually contained several mitochondria (not shown). They had the morphological appearance of terminals formed by the local axon collaterals of the SNr output neurons (Damlama, M., Bolam, J.P. & Tepper, J.M. *Soc. Neurosci. Abstr.* 19, 1432, 1993) and were present only in those animals in which the tracer injections also gave rise to retrograde labeling in SNr. In summary, the electron microscopic data indicate that most of the synaptic terminals located in SNc were anterogradely labeled from the SC. Of these, the majority made asymmetric contacts with both TH-positive and TH-negative elements, although TH-negative contacts predominated.

Retrograde tract tracing

To identify cells in the SC that give rise to direct tectonigral fibers, we injected small quantities (10 nl) of the retrograde tracer cholera toxin subunit B into the SNc. The tissue was also processed to reveal TH-immunoreactive structures (Fig. 1e,f). We found a relatively uniform population of small retrogradely labeled cells (mean diameter = 10.78 \pm 0.48 μ m) concentrated in the intermediate layers of the SC, although scattered cells were also observed in the adjacent deep and optical layers (Figs. 1g and 3b). The discovery of retrogradely labeled cells in different layers of the colliculus supports the anterograde tracing data and raises the possibility that the tectonigral projection might have several functionally diverse components.

Tectonigral projection topography

Tracer injections involving lateral aspects of the SC always produced more intense anterograde labeling in the ventral midbrain than did more medial injections (Fig. 3a). Quantitative analysis of antero-

gradely labeled boutons in the SNc confirmed that laterally located tracer injections were associated with significantly more boutons in all sampled regions (ANOVA main effect of injection site: $F_{1,5} = 8.83$; $P = 0.031$; Table 1). The analysis also revealed a medial-medial, lateral-lateral topography within the tectonigral projection (Table 1); lateral injections were associated with higher concentrations of boutons in lateral sections of SNc, whereas boutons labeled from medial injections were more dense in medial SNc (ANOVA interaction between injection site and SNc region: $F_{1,5} = 10.1$; $P = 0.025$).

Two cases were selected from a series of injections ($n = 7$) in which the retrograde tracer was largely confined either to medial or lateral SNc (Fig. 3b). In these two examples, retrograde labeling was essentially distributed within medial and lateral sectors of the SC. This result confirms a partially overlapping, medial-medial, lateral-lateral topography in the tectonigral projection.

In summary, our light and electron microscopic data reveal a direct projection from the SC to SNc, which is in a position to transmit short-latency sensory information throughout dopamine-containing regions of the ventral midbrain. To test this hypothesis, we conducted a series of electrophysiological experiments to determine whether the SC acts as a critical relay for short-latency components of visual-evoked field potentials recorded locally in the SNc.

Electrophysiological experiments

We first determined the relative latencies of visually evoked potentials (VEPs) recorded simultaneously from the superficial layers of the SC and the SNc of urethane-anesthetized rats. Field potential signal averaging revealed short-latency flash-evoked responses in both structures (Fig. 4). Initial onset and peak latencies were reliably shorter for VEPs recorded from the SC, as would be predicted if the colliculus acts as relay for visual information destined for the ventral midbrain.

If the SC is a critical relay for short-latency visual signals, local manipulations of collicular neurotransmission should produce appropriate modulations of nigral VEPs. Disinhibitory microinjec-

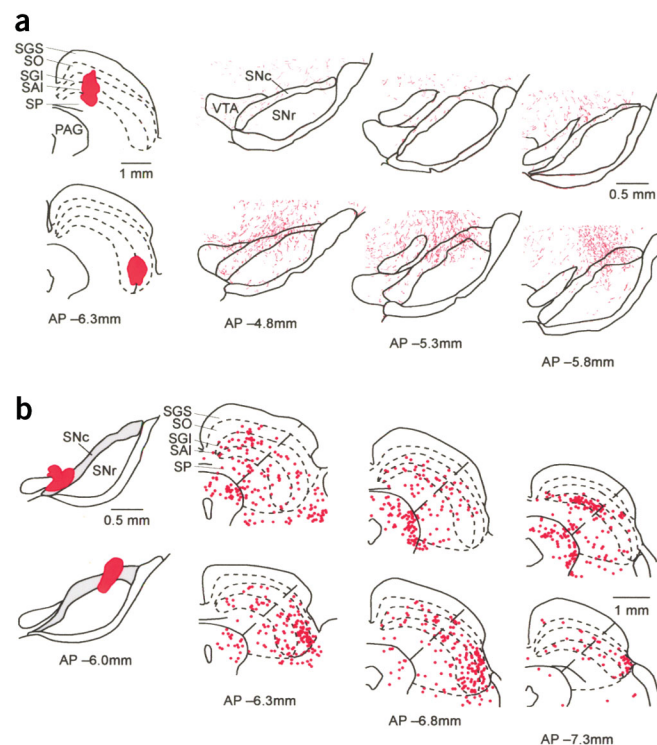


Figure 3 Tectonigral projection topography. (a) Drawing of injection sites of the anterograde tracer BDA in medial (top) and lateral (bottom) intermediate layers of the SC. Transported label associated with each of the injections is plotted on the two adjacent series of nigral sections. Note the higher density of labeling associated with the lateral collicular injection. (b) Injection sites of the retrograde tracer CTb in the medial (top) and lateral (bottom) SNc are shown with their respective series of coronal collicular sections illustrating the location of retrogradely labeled cells. Summing over the illustrated sections, the total number of retrogradely labeled cells contained within the medial and lateral sectors of the SC (separated by diagonal lines) were 143 and 134 for the medial nigral injection, and 74 and 256 for the lateral nigral injection ($\chi^2 = 55.9$; $P < 0.0001$). See Fig. 1 legend for abbreviations in collicular layers and substantia nigra; VTA, ventral tegmental area.

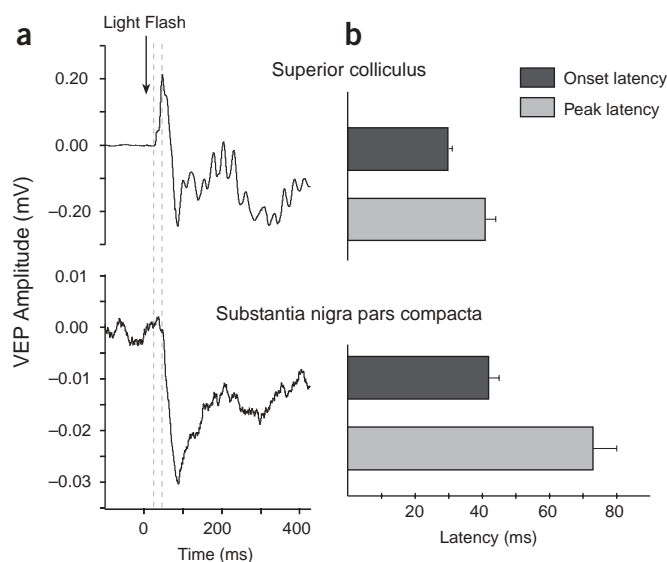


Figure 4 Response latencies of visual-evoked field potentials in the SC and the SNc. **(a)** A typical example of collicular and nigral VEPs from an individual subject. The two dotted lines indicate initial onset and peak latencies, respectively, for the collicular VEP. **(b)** Group data ($n = 12$) showing that both the mean onset latencies ($F_{1,11} = 11.64$; $P = 0.0058$) and peak latencies ($F_{1,11} = 36.44$; $P < 0.0001$) were significantly shorter for collicular VEPs.

tions of a GABA antagonist, bicuculline, adjacent to the collicular recording electrode increased the amplitude of local VEPs, and the VEP responses recorded from the SNc (Fig. 5). Conversely, both collicular and nigral VEPs were reliably decreased by collicular microinjections of the local anesthetic lidocaine (Fig. 5). These results establish the SC as a powerful regulator of short-latency visual input to the SNc.

Finally, we tested whether the integrity of the SC is essential for the transmission of visual information to the SNc. Baseline VEPs were recorded from both collicular and nigral electrodes. Subsequent aspiration of ipsilateral visual cortex (Fig. 6a) confirmed the powerfully suppressive effect (Fig. 6c,d) that unilateral cortical ablation has on collicular visual processing, which has been reported widely by others^{21–23}. We noted, however, that cortical ablations also induced a correlated suppression of visual processing in SNc (Fig. 6c,d). Since the application of bicuculline to the SC can reverse the inhibitory effects of cortical lesions²⁴ and potentiate local VEPs (this study), we applied a swab soaked in bicuculline to the surface of the SC exposed by the cortical ablation. In the complete absence of ipsilateral visual cortex, the bicuculline rapidly re-instated VEPs recorded both locally in the SC and in the substantia nigra (Fig. 6c,d). As a final step, the superficial layers of the SC were removed by aspiration. All visually evoked

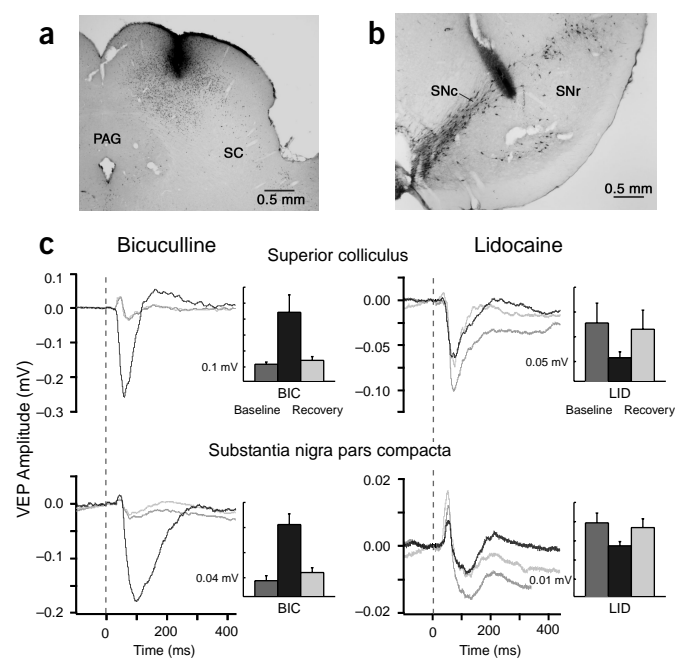
activity in the substantia nigra was abolished by this treatment, even when the bicuculline swab was returned to the exposed surface of the collicular intermediate layers (Fig. 6c). This final treatment ruled out the possibility that the previous reinstatement of collicular and nigral VEPs by bicuculline was mediated by cortical and/or hippocampal tissue exposed by the aspiration, or by diffusion into the ventricles. These results effectively dissociate the potential involvement of cortical and midbrain visual systems in the provision of short-latency visual input to the SNc.

DISCUSSION

The present study establishes a direct projection from a primary sensory structure, the SC, to dopamine containing regions of the ventral midbrain, and that the integrity of the SC is critical for the transmission of short latency visual information to the SNc. This establishes the retino-tecto-nigral circuit as the most likely source of short latency visual input to the ventral midbrain.

Several lines of evidence suggest that the tectonigral pathway may have several functionally distinguishable components that make contact with both dopaminergic and non-dopaminergic neurons in the substantia nigra and the ventral tegmental area. First, our electron-microscopy data revealed that tectonigral boutons form both asymmetric (presumed excitatory) and symmetric (presumed inhibitory) synapses with TH-positive and TH-negative elements in SNc. It is likely that the different types of contact originate from different cell populations in the SC. This supposition is consistent with the observation of retrogradely labeled neurons located in different layers of the SC (Fig. 3b). Anatomical, physiological and behavioral analyses of the SC suggest a modular architecture²⁵

Figure 5 Microinjections into the SC modulate VEPs both locally and in the SNc. **(a)** The black dots surrounding a typical injection site in the SC shows Fos-like immunoreactivity induced by a microinjection of bicuculline. This index of neural excitation⁴¹ suggests the direct disinhibitory action of bicuculline was generally confined within the boundaries of the SC. **(b)** A typical example of a recording site located in the SNc. Tyrosine hydroxylase-positive dopaminergic neurons appear black. **(c)** Individual and group data showing that injections of bicuculline ($n = 7$) increased the mean amplitudes of VEPs in the SC ($F_{2,6} = 7.29$; $P = 0.0084$) and the SNc ($F_{2,6} = 19.72$; $P = 0.0002$), whereas injections of lidocaine ($n = 7$) reduced VEP amplitude in both the SC ($F_{2,6} = 3.98$; $P = 0.047$) and the SNc ($F_{2,6} = 6.29$; $P = 0.0136$). The dark gray traces and histogram bars represent pre-drug VEPs; the black traces and bars indicate VEPs recorded immediately after drug administration; and the light gray traces and bars show the VEPs recorded after the effects of the drugs had dissipated. Abbreviations: BIC, bicuculline; LID, lidocaine; PAG, periaqueductal grey; SC, superior colliculus; SNc substantia nigra pars compacta; SNr substantia nigra pars reticulata.



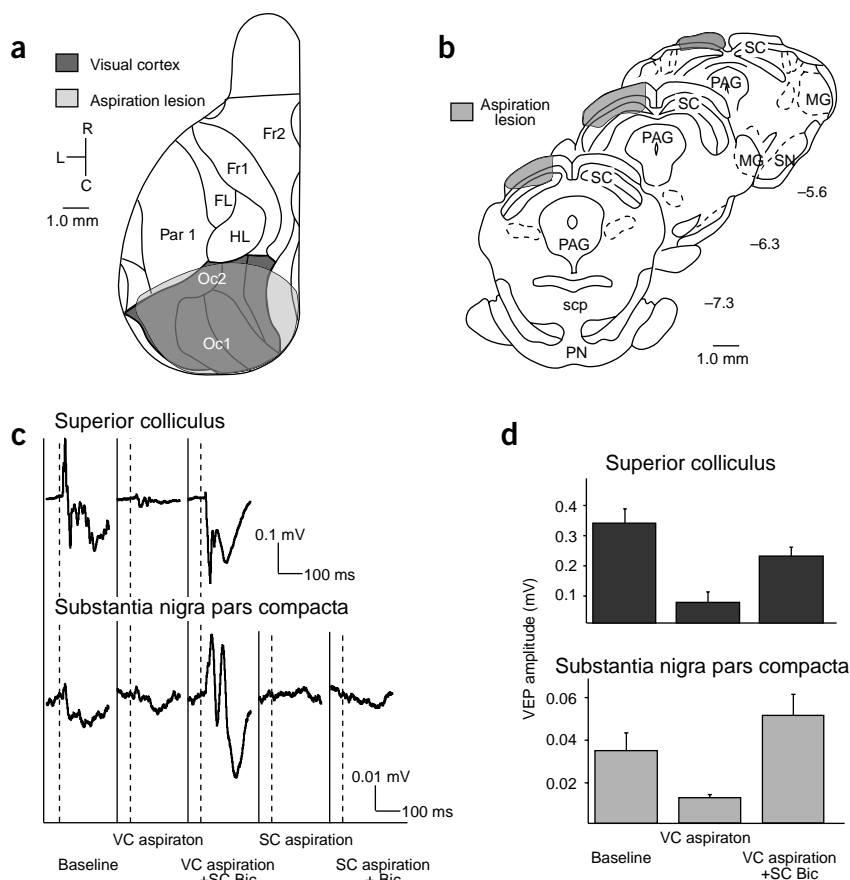


Figure 6 Effect of visual system aspiration lesions on visual evoked responses. **(a)** A typical unilateral aspiration lesion of visual cortex represented on a surface plot of cerebral cortex modified from the atlas of Zilles⁴². **(b)** A representative aspiration lesion of the superficial layers of the SC plotted on coronal sections modified from the atlas of Paxinos and Watson⁴³. **(c)** A sequence of lesion and pharmacological treatments modulate VEP amplitudes recorded from the SC and the SNc of a single subject. Dotted lines indicate the time of the light flash. **(d)** Group data ($n = 4$) showing that aspiration of visual cortex reliably suppressed VEP amplitudes in both the SC ($F_{2,3} = 17.2$; $P = 0.0032$) and the substantia nigra ($F_{2,3} = 6.45$; $P = 0.032$). After the topical administration of bicuculline to the SC, VEPs in either structure did not differ reliably from baseline values. Aspiration of collicular superficial layers, with and without topical application of bicuculline, completely abolished visual responses in the SNc. Abbreviations: Bic, bicuculline; FL, forelimb area; Fr1 and 2, frontal cortical areas 1 and 2; HL, hindlimb area; MG, medial geniculate nucleus; Oc1 and 2, occipital cortex areas 1 and 2; Par 1, parietal cortex area 1; PAG, periaqueductal gray; PN, pons; SC, superior colliculus; scp, superior cerebellar peduncle; SN, substantia nigra; VC, visual cortex.

in which multimodal sensory¹⁶ and contextual inputs from cortical^{25,26} and limbic^{27,28} sources are directed to anatomically and functionally dissociable output channels^{15,25,29}. Many of these functional units are differentially distributed both within and across the laminar structure of the colliculus²⁵. It is therefore likely that tectonigral cells of origin in different collicular regions will be subject to qualitatively different influences. This conclusion is supported by our recent electrophysiological study¹⁹ showing that local disinhibitory chemical activation of the SC can have either excitatory or inhibitory effects both on putative dopaminergic and non-dopaminergic neurons recorded in the ventral midbrain.

The discovery of possible excitatory and inhibitory components in a direct tectonigral projection suggests that the pathway may mediate both the positive and negative modulation of dopaminergic neurons at short latency². Activation could be achieved by relevant pre-attentive visual signals being directed to components of the tectonigral projection that have direct or indirect excitatory effects on dopaminergic neurons. Alternatively, abundant afferent connections to the SC from regions of the brain associated with expectation (cortex³⁰ and basal ganglia³¹) and timing (basal ganglia and cerebellum^{32,33}) suggest that sufficient information may be present in the SC to enable the absence of an expected event also to be detected at short latency. The direction of such a signal to components of the tectonigral projection that have direct or indirect inhibitory effects could be responsible for the temporary suppression of dopaminergic neuronal activity observed shortly after the omission of an expected reward².

The perceptual properties of the retino-tecto-nigral projection and related circuitry will largely determine how much detail can be discriminated to form pre-attentive stimulus classifications. It therefore

remains to be discovered whether such circuitry has the capacity to distinguish unpredictable reward or reward-related stimuli (necessary for hypothesized reward prediction error signals in associative learning⁹) from the wider class of unpredictable, biologically salient events that interrupt ongoing behavior and attract orienting responses (sufficient for attention-related hypotheses of dopaminergic activation^{6,34}). The distinction between these two suppositions is neatly captured in the lines by Thomas Gray (1716–1771): “Not all that tempts your wand’ring eyes and heedless hearts, is lawful prize; Nor all, that glisters, gold.” To date, available experimental evidence^{2,7} suggests that dopaminergic neurons will signal all that ‘glisters’ including ‘gold’—which may diminish their capacity to report accurate reward prediction errors.

METHODS

All aspects of this study were performed with Home Office approval under section 5(4) of the Animals (Scientific Procedures) Act of 1986, and experimental protocols received prior approval of the institutional ethics committees.

Tracer injections. For the light microscopy experiments, we used 38 female Hooded Lister rats (280–350 g) bred in the Sheffield laboratory. Animals were anesthetized with xylazine (0.34 mg/kg, Bayer plc) and ketamine (0.76 mg/kg, Fort Dodge Animal Health Ltd.). Tracers were injected unilaterally into the SC (AP 6.0–6.8 mm, bregma; ML 0.5–2.5 mm, bregma; DV 3.7–4.5 mm, dura) or the SNc (AP 5.0–5.8 mm, bregma; ML 1.0–3.0 mm, bregma; DV 8.0–9.0 mm, dura). Pressure injections (40–60 nl) of biotinylated dextran amine (BDA, 10% in phosphate buffer) and iontophoretic injections of *Phaseolus vulgaris* leucoagglutinin (PHA-L; 5 μ A positive current applied to a 2.5% solution in phosphate buffer; 7 s on, 7 s off for 20 min) were made into the SC. Pressure injections (10 nl) of cholera toxin subunit b (CTb; 1% in phosphate buffer) were made into the SNc.

For the electron microscopic analysis, an additional four rats received pressure deposits (40–60 nl) of BDA in the SC, and five male Sprague-Dawley rats (250–300 g, Charles River, Margate, Kent, UK), anesthetized by a mixture of

fenentanyl/fluonisonone (0.135 and 10 mg/ml, respectively; Hypnorm, Janssen-Cilag Ltd.) and midazolam (5 mg/ml; Hypnovel, Roche Products Ltd.) in a ratio of 1:1:2 with sterile water (2.7 ml/kg), received unilateral iontophoretic deposits of PHA-L (2.5% in 0.01 M PB, pH 8.0) using the same injection parameters as described above. After surviving for 7 d, all animals were anesthetized with pentobarbitone and perfused transcardially with warmed saline (40 °C) or phosphate-buffered saline (0.01 M phosphate; PBS), followed by 4% paraformaldehyde in phosphate buffer (pH 7.4; PB) for light microscopy or 3% paraformaldehyde plus 0.1% glutaraldehyde for electron microscopy. Serial coronal or sagittal sections (50–70 µm) of the midbrain were cut on a vibrating microtome and collected in PB or PBS.

Light microscopy: histology. To reveal the tracers (BDA, PHA-L or CTb), free-floating sections were washed with 0.1M PB followed by 0.1M PB containing 0.3% Triton X-100 (PB-TX) for 20 min, and then processed according to previously described procedures³⁵. Briefly, for animals injected with PHA-L or CTb, the sections were incubated overnight in primary antibody solution (goat anti-PHA-L, 1:1,000 dilution, Vector, or goat anti-CTb, 1:4,000 dilution, Quadrantech). The next day, sections were washed with PB-TX and incubated for 2 h in biotinylated rabbit anti-goat IgG (1:100, Vector), in PB-TX containing 2% normal rabbit serum. All sections were then incubated in Elite Vectastain ABC reagent (Vector; 1:100 in PB-TX) for 2 h. The peroxidase associated with the tracers (PHA-L, BDA and CTb) was revealed by reacting tissue with H₂O₂ for ~1 min using nickel-enhanced diaminobenzidine (DAB) as the chromogen³⁶. Sections were then transferred to a blocking solution (PB containing 2.5% BSA, 2% normal horse serum and 0.3% Triton X-100) for 2 h. Tissue was then incubated with a mouse monoclonal antibody (1:3,000 dilution) raised against tyrosine hydroxylase (TH, Boehringer Mannheim) and exposed to biotinylated horse anti-mouse IgG (1:1,000 dilution, Vector) and then the Elite Vectastain ABC reagent (1:200, Vector). TH immunoreactivity was revealed by incubation with Vector VIP (Vector) as the chromogen. A separate series of sections were incubated with a rabbit polyclonal antibody (1:5,000 dilution) raised against Fos protein (Autogen Bioclear Ltd.). The secondary antibody was biotinylated anti-rabbit made in goat (1:100 dilution, Vector) and then the Elite Vectastain ABC reagent (1:50, Vector). Fos-like immunoreactivity was revealed by exposure to DAB as the chromogen. Finally, sections were washed in distilled water, mounted on gelatine-coated slides, dehydrated in graded dilutions of alcohol, cleared in xylene and coverslipped in DPX.

Light microscopy: data analysis. Bright- and dark-field optics were used to observe the immunolabeling associated with the transported tracers and TH. The distribution of both anterograde and retrograde markers (Fig. 3) was plotted with a camera lucida attachment to the microscope. Anterograde transport of BDA was quantified by counting the boutons contained within a series of four 300-µm diameter fields (400× magnification), distributed evenly along the rostro-caudal plane of the SNc. In seven cases, the SNc in two sections (~1.5 mm and ~3.0 mm lateral) were analyzed. Statistical reliability was assessed with a three-factor ANOVA with medial ($n = 3$) versus lateral ($n = 4$) collicular injection site as a between-subjects variable. Two repeated-measures factors were medial versus lateral nigral section (2 levels) and the rostro-caudal measurement positions within SNc (4 levels).

Electron microscopy: histology and analysis. Tissue for the electron microscopic analysis was treated in a similar manner, except that the sections were freeze-thawed using isopentane and liquid nitrogen, and Triton X-100 was not used. Tracers were revealed using DAB as the chromogen for the peroxidase reactions. Sections were incubated to reveal TH immunoreactivity by the peroxidase-antiperoxidase method using a mouse anti-TH antibody (dilution 1:20,000, Sigma) and revealed using tetramethylbenzidine/tungstate as the chromogen for the peroxidase reaction^{37,38}. After post-fixation in osmium tetroxide (1% in PB containing 5% glucose), they were embedded in resin and flat-mounted on microscope slides³⁹. Regions of the SNc in which anterogradely labeled and TH-positive structures intermingled were re-embedded and re-sectioned for electron microscopic analysis. The sections were collected on Pioloform-coated, single-slot grids that were stained with lead citrate and examined in a Philips CM10 or CM100 electron microscope.

Electrophysiology. For the electrophysiological experiments, we used 23 male Hooded Lister rats (400–650 g). Animals were anesthetized with urethane (ethyl carbamate, 1.25 g/kg), and atropine methyl nitrate (6 mg/kg) was administered to reduce mucus secretion. A contralateral approach using an angle of 25° (2.0–3.0 mm, lateral) was used to position a parylene-C-insulated tungsten microelectrode (1–2 MΩ) into the SNc (AP 5.2–5.6 mm, bregma). A second electrode, sometimes joined with a 50 µm diameter glass injection pipette filled with bicuculline methiodide (40 ng per 400 nl saline) or lidocaine (40 µg per µl of distilled water; Sigma), was introduced vertically into the SC (5.8–6.8 mm, bregma; 1.0–2.0 mm, lateral; 3.5–5.0 mm, dura). Averaged visual evoked potentials (VEPs) were recorded simultaneously on both electrodes in response to 300 whole-field flashes (0.5 Hz, 10 ms duration, 60 LUX green LED 570 nm, positioned 5 mm from the contralateral eye); these parameters were maintained throughout all electrophysiological experiments. Field potentials were amplified, band-pass filtered (DC–1 kHz, 3 dB points), digitized at 10 kHz and recorded directly to computer disk using a 1401+ data acquisition system (CED Systems). Signal averaging was performed by CED Spike 2 software. Using averaged VEPs, onset latencies were defined as the point of intersection of a line of best fit through the 0.5 s of data immediately prior to the flash onset, and a line connecting the 20- and 80-percentile points in the leading edge of the first peak in the VEP trace (compare to Fig. 1 in ref. 40). Injections of bicuculline and lidocaine were made at a rate of 0.5 µl/min. Aspiration lesions were performed with a blunted 20-g hypodermic needle connected to a vacuum pump. A Gelfoam swab soaked in a solution of bicuculline methiodide (100 µg/ml) was placed directly onto the exposed SC.

The effects of these treatments on VEP magnitude were determined by calculating the difference (mV) between the maximum and minimum deflections of the averaged VEP trace during the 500 ms following stimulus onset. Measures of VEP latency and magnitude were analyzed by single-factor and repeated-measures analyses of variance.

ACKNOWLEDGMENTS

This work was supported by a Fundação de Amparo à Pesquisa do Estado de São Paulo grant (97/10490-0 to E.C.), Wellcome Trust grants to P.R. (059735, 068012) and P.O. (062742), and Medical Research Council support for J.P.B. and J.B. (MRC Studentship). The authors are grateful to J. McHaffie for his comments on early drafts of the manuscript, to N. Walton for histological assistance and to P. Furness for help with data analysis.

COMPETING INTERESTS STATEMENT

The authors declare that they have no competing financial interests.

Received 28 April; accepted 24 June 2003

Published online at <http://www.nature.com/natureneuroscience/>

- Overton, P.G. & Clark, D. Burst firing in midbrain dopaminergic neurons. *Brain Res. Rev.* **25**, 312–334 (1997).
- Schultz, W. Predictive reward signal of dopamine neurons. *J. Neurophysiol.* **80**, 1–27 (1998).
- Freeman, A.S. Firing properties of substantia nigra dopaminergic neurons in freely moving rats. *Life Sci.* **36**, 1983–1994 (1985).
- Guarraci, F.A. & Kapp, B.S. An electrophysiological characterization of ventral tegmental area dopaminergic neurons during differential pavlovian fear conditioning in the awake rabbit. *Behav. Brain Res.* **99**, 169–179 (1999).
- Horvitz, J.C., Stewart, T. & Jacobs, B.L. Burst activity of ventral tegmental dopamine neurons is elicited by sensory stimuli in the awake cat. *Brain Res.* **759**, 251–258 (1997).
- Redgrave, P., Prescott, T.J. & Gurney, K. Is the short latency dopamine response too short to signal reward error? *Trends Neurosci.* **22**, 146–151 (1999).
- Horvitz, J.C. Mesolimbocortical and nigrostriatal dopamine responses to salient non-reward events. *Neuroscience* **96**, 651–656 (2000).
- Waelti, P., Dickinson, A. & Schultz, W. Dopamine responses comply with basic assumptions of formal learning theory. *Nature* **412**, 43–48 (2001).
- Schultz, W. Getting formal with dopamine and reward. *Neuron* **36**, 241–263 (2002).
- Schultz, W. & Dickinson, A. Neuronal coding of prediction errors. *Annu. Rev. Neurosci.* **23**, 473–500 (2000).
- Bar-Gad, I. & Bergman, H. Stepping out of the box: information processing in the neural networks of the basal ganglia. *Curr. Opin. Neurobiol.* **11**, 689–695 (2001).
- Fiorillo, C.D., Tobler, P.N. & Schultz, W. Coding of reward uncertainty by sustained activation of dopamine neurons. *Science* **299**, 1898–1902 (2003).
- Schneider, G.E. Two visual systems. *Science* **163**, 895–901 (1969).
- Thorpe, S.J. & Fabre-Thorpe, M. Seeking categories in the brain. *Science* **291**, 260–263 (2001).
- Dean, P., Redgrave, P. & Westby, G.W.M. Event or emergency? Two response systems

- in the mammalian superior colliculus. *Trends Neurosci.* **12**, 137–147 (1989).
16. Stein, B.E. & Meredith, M.A. *The Merging of the Senses* (The MIT Press, Cambridge, Massachusetts, 1993).
 17. Jay, M.F. & Sparks, D.L. Sensorimotor integration in the primate superior colliculus. *J. Neurophysiol.* **57**, 22–34 (1987).
 18. Wurtz, R.H. & Goldberg, M.E. The primate superior colliculus and the shift of visual attention. *Invest. Ophthalmol.* **11**, 441–450 (1972).
 19. Coizet, V., Comoli, E., Westby, G.W.M. & Redgrave, P. Phasic activation of substantia nigra and the ventral tegmental area by chemical stimulation of the superior colliculus: an electrophysiological investigation in the rat. *Eur. J. Neurosci.* **17**, 28–40 (2003).
 20. Gonzalez-Hernandez, T. & Rodriguez, M. Compartmental organization and chemical profile of dopaminergic and GABAergic neurons in the substantia nigra of the rat. *J. Comp. Neurol.* **421**, 107–135 (2000).
 21. Sprague, J.M. Interaction of cortex and superior colliculus in the mediation of visually guided behavior in the cat. *Science* **153**, 1544–1547 (1966).
 22. Goodale, M.A. Cortico-tectal and intertectal modulation of visual responses in the rat's superior colliculus. *Exp. Brain Res.* **17**, 75–86 (1973).
 23. Hardy, S.C. & Stein, B.E. Small lateral suprasylvian cortex lesions produce visual neglect and decreased visual activity in the superior colliculus. *J. Comp. Neurol.* **274**, 527–542 (1988).
 24. Ciaramitaro, V.M., Todd, W.E. & Rosenquist, A.C. Disinhibition of the superior colliculus restores orienting to visual stimuli in the hemianopic field of the cat. *J. Comp. Neurol.* **387**, 568–587 (1997).
 25. Mana, S. & Chevalier, G. Honeycomb-like structure of the intermediate layers of the rat superior colliculus: Afferent and efferent connections. *Neuroscience* **103**, 673–693 (2001).
 26. Tsumori, T., Yokota, S., Ono, K. & Yasui, Y. Organization of projections from the medial agranular cortex to the superior colliculus in the rat: a study using anterograde and retrograde tracing methods. *Brain Res.* **903**, 168–176 (2001).
 27. Cameron, A.A., Khan, I.A., Westlund, K.N., Cliffer, K.D. & Willis, W.D. The efferent projections of the periaqueductal gray in the rat: a *Phaseolus vulgaris* leucoagglutinin study. I. Ascending projections. *J. Comp. Neurol.* **351**, 568–584 (1995).
 28. Heilman, K.M. Emotion and the brain: a distributed modular network mediating emotional experience. in *Neuropsychology* (ed. Zaidel, D.W.) 139–158 (Academic, San Diego, 1994).
 29. Redgrave, P., Westby, G.W.M. & Dean, P. Functional architecture of rodent superior colliculus: relevance of multiple output channels. in *Progress in Brain Research* (eds. Hicks, T.P., Molotchnikoff, S. & Ono, T.) 69–77 (Elsevier, Amsterdam, 1993).
 30. Basso, M.A. Cognitive set and oculomotor control. *Neuron* **21**, 665–668 (1998).
 31. Hikosaka, O., Sakamoto, M. & Usui, S. Functional properties of monkey caudate neurons III. Activities related to expectation of target and reward. *J. Neurophysiol.* **61**, 814–831 (1989).
 32. Wittmann, M. Time perception and temporal processing levels of the brain. *Chronobiol. Int.* **16**, 17–32 (1999).
 33. Dreher, J.C. & Grafman, J. The roles of the cerebellum and basal ganglia in timing and error prediction. *Eur. J. Neurosci.* **16**, 1609–1619 (2002).
 34. Redgrave, P., Prescott, T. & Gurney, K.N. The basal ganglia: A vertebrate solution to the selection problem? *Neuroscience* **89**, 1009–1023 (1999).
 35. Hsu, S.M., Raine, L. & Fanger, H. The use of antiavidin antibody and avidin-biotin-peroxidase complex in immunoperoxidase techniques. *Am. J. Clin. Pathol.* **75**, 816–821 (1981).
 36. Adams, J.C. Biotin amplification of biotin and horseradish peroxidase signals in histochemical stains. *J. Histochem. Cytochem.* **40**, 1457–1463 (1992).
 37. Clarke, N.P., Bolam, J.P. & Bevan, M.D. Glutamate-enriched inputs from the mesopontine tegmentum to the entopeduncular nucleus in the rat. *Eur. J. Neurosci.* **8**, 1363–1376 (1996).
 38. Weinberg, R.J. & Veneyck, S.L. A tetramethylbenzidine/tungstate reaction for horseradish peroxidase histochemistry. *J. Histochem. Cytochem.* **39**, 1143–1148 (1991).
 39. Bolam, J.P. Preparation of CNS tissue for light and electron microscopy. in *Experimental Neuroanatomy: a Practical Approach* (ed. Bolam, J.P.) 1–29 (Oxford Univ. Press, Oxford, 1992).
 40. Matsuura, T. *et al.* CBF change evoked by somatosensory activation measured by laser-Doppler flowmetry: independent evaluation of RBC velocity and RBC concentration. *Jpn. J. Physiol.* **49**, 289–296 (1999).
 41. Sagar, S.M., Sharp, F.R. & Curran, T. Expression of c-fos protein in brain: Metabolic mapping at the cellular level. *Science* **240**, 1328–1331 (1988).
 42. Zilles, K. Anatomy of the neocortex: cytoarchitecture and myeloarchitecture. in *Cerebral Cortex of the Rat* (eds. Kolb, B. & Tees, R.C.) 77–112 (MIT Press, Cambridge, Massachusetts, 1990).
 43. Paxinos, G. & Watson, C. *The Rat Brain in Stereotaxic Coordinates* (Academic, Sydney, 1986).